

Research Note

Characteristics of the Interstellar Medium as Deduced from Low-frequency Recombination Line Observations

P. A. Shaver*

Raman Research Institute, Bangalore, India

Received June 3, revised August 4, 1975

Summary. Upper limits on the intensities of recombination lines below 200 MHz imply upper limits on the filling factor for the cold cloud component of the interstellar medium of ≈ 0.005 – 0.05 , depending on the temperature assumed; for the gas responsible for the observed low-frequency continuum absorption in Sgr A

and W49B they imply lower limits on the electron density of 0.2 – 2 cm^{-3} .

Key words: radio recombination lines — interstellar medium — cold cloud component

I. Introduction

The recombination line spectrum below 200 MHz should be dominated by contributions from the low-density gas of the interstellar medium. (“Density” refers to electron density throughout this paper.) The strongest lines should be those due to negative absorption in cold, low-density gas of radiation from strong, distant nonthermal galactic sources [Shaver (1975), hereinafter referred to as Paper I].

The “excess” temperature at the line frequency can be written

$$\begin{aligned} \Delta T_L = T_O [e^{-\tau_C}(e^{-\tau_L} - 1)] \\ + T_e \left[\left(\frac{b_m \tau_L^* + \tau_C}{\tau_L + \tau_C} \right) (1 - e^{-(\tau_L + \tau_C)}) - (1 - e^{-\tau_C}) \right] \\ + T_M \left[\frac{1 - e^{-(\tau_L + \tau_C)}}{\tau_L + \tau_C} - \frac{1 - e^{-\tau_C}}{\tau_C} \right], \end{aligned} \quad (1)$$

where T_O is the main beam brightness temperature due to a source located behind the gas, T_M is that due to the distributed galactic nonthermal emission, and T_e is the electron temperature of the gas. This equation assumes that both source and beam are uniformly covered by the interstellar component under consideration. The line and continuum opacities are given by

$$\tau_L = \frac{518 EM}{v \Delta V_L T_e^{5/2}} b_n \left[1 - 20.8 \frac{T_e}{v} \frac{d \ln b_n}{dn} \right], \quad (2)$$

* Present address: Kapteyn Astronomical Institute, University of Groningen.

and

$$\tau_C = \frac{0.0314 EM}{v^2 T_e^{3/2}} f [1.5 \ln T_e - \ln(20.2v)], \quad (3)$$

respectively (Paper I, Oster, 1961), where the units are EM (pc cm^{-6}), v (GHz), ΔV_L (km/s), and T_e ($^{\circ}\text{K}$). Equation (2) refers to the line centre of Doppler-broadened α -lines, and the following two assumptions have been made: $N_{\text{H}^+} = 0.9 N_e$, and $n \gg 1$; τ_L^* is the equilibrium value of τ_L . In Eq. (3), f is a correction factor to Oster’s classical approximation; it is very close to unity for the low frequencies of interest here (Gayet, 1970; Oster, 1970).

If the resolution is adequate at low frequencies, the first term in Eq. (1) may be dominant, and the line-to-continuum temperature ratio can then be written

$$\frac{\Delta T_L}{T_O} = e^{-\tau_C}(e^{-\tau_L} - 1). \quad (4)$$

This fraction can exceed unity (negative τ_L) if the path length through cold clouds in the interstellar medium is substantial, whereas for the hot intercloud component alone it is unlikely to exceed a few percent (Fig. 1). Low frequency line observations are therefore of interest in elucidating the properties of the cold cloud component in particular.

A few years ago Turner *et al.* (1970) and Heiles and Turner (1971) incidentally observed the frequencies of the $\text{H}307\alpha$ and $\text{H}389\alpha$ recombination lines (226 and 111 MHz respectively) in searches for interstellar NO

and SH in the directions of discrete radio sources. The frequency resolution was high (1–2 kHz), and their observations permit significant limits to be placed on the filling factor and electron density of the cold gas in the interstellar medium.

II. The Cold Cloud Component

Table 1 lists four of the sources observed by Turner *et al.* (1970) and Heiles and Turner (1971). The upper limit for ΔT_L is shown as a fraction of T_0 (i.e. for the discrete source alone) at the same frequency; T_0 was obtained by extrapolation from measurements at higher frequencies and summarised by Maxwell and Taylor (1968) and Milne (1970). These ratios can be used together with Fig. 1 to give upper limits on the path lengths (d) through cold clouds along the lines of sight to the four sources. This procedure assumes that the T_0 term in Eq. (1) is dominant, an assumption which is clearly not true for the large beamwidths (\gtrsim one degree) used in these observations; however it is conservative insofar as it weakens the limits which can be placed on the filling factor, because the other two terms in Eq. (1) must also contribute in some measure to the line intensity whereas only T_0 has been included in the

Table 1. Derived filling factors for the cold cloud component of the interstellar medium

Source	$\Delta T_L/T_0$ (111 MHz)	$\Delta T_L/T_0$ (226 MHz)	D (kpc)	η ($T_e=20^\circ\text{K}$)	η ($T_e=100^\circ\text{K}$)
Sgr A	<0.063	—	10	<0.008	<0.07
W44	<0.018	—	3	<0.007	<0.07
W49	<0.080	<0.087	10	<0.010	<0.09
W51	<0.014	<0.018	5	<0.003	<0.03

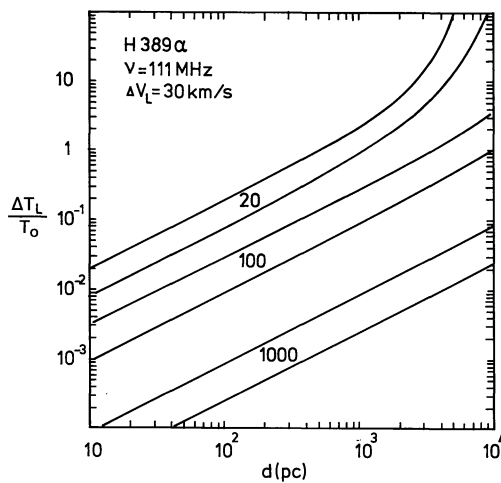


Fig. 1. The H389 α line amplification factor computed from Eqs. (2)–(4) for $\Delta V_L = 30$ km/s, plotted against the path length through the line-emitting medium for three values of electron temperature, 20, 100 and 1000 °K. For each temperature two values of electron density have been used; the upper and lower curves correspond to $N_e = 0.1$ and 0.05 cm^{-3} respectively

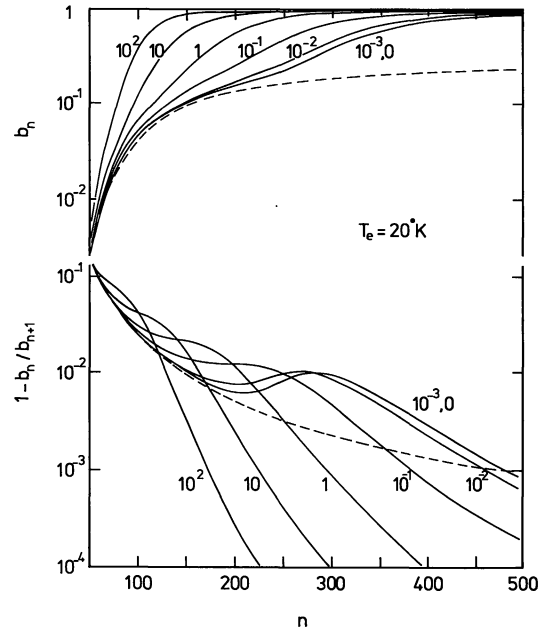


Fig. 2. b_n factors from Paper I, which include the effects of the galactic radiation field, plotted against principal quantum number for $T_e = 20^\circ\text{K}$ and the densities indicated. The dashed curve represents the zero-density case with no radiation field present

denominator in Eq. (4). A more comprehensive treatment is discussed below. Theoretical b_n -values must be used which incorporate the effects of the galactic non-thermal radiation field, which is the dominant factor in determining the high atomic level populations in low-density plasmas; the values from Paper I have been used in computing the curves in Fig. 1. For convenience the b_n -factors for $T_e = 20^\circ\text{K}$ from Paper I are reproduced in Fig. 2. It should be noted that these b_n -factors are essentially independent of the ionising mechanism, except via the electron temperature and density. The distance (D) necessary to convert the path lengths to filling factors ($\eta = d/D$) were taken from Radhakrishnan *et al.* (1972) and Wilson (1973), and are listed in Table 1.

The results are shown in Table 1 for the density (0.05 cm^{-3}) and temperature (20–100 °K) thought to characterize the cold cloud component of the interstellar medium (Field *et al.*, 1969; Hjellming *et al.*, 1969). Generally $\eta < 0.007$ for $T_e = 20^\circ\text{K}$ and $\eta < 0.06$ for $T_e = 100^\circ\text{K}$. If a somewhat higher density is assumed, the filling factor becomes even smaller: for $N_e = 0.1 \text{ cm}^{-3}$, $\eta < 0.003$ for $T_e = 20^\circ\text{K}$ and $\eta < 0.02$ for $T_e = 100^\circ\text{K}$ [pressure broadening becomes important only for densities above 25 cm^{-3} (Paper I), and so plays no role here]. The maximum likely velocity dispersion is about 100 km/s; using this figure and $N_e = 0.05 \text{ cm}^{-3}$ the upper limits on η are found to be 0.02 and 0.20 for $T_e = 20^\circ\text{K}$ and 100°K respectively. These limits both imply $\tau_C < 0.08$ for a total line of sight of 10 kpc; by contrast the work of Dulk and Slee (1975) indicates 111 MHz optical depths of 0.22 and 2.9 for

W49B and Sgr A respectively. It is therefore clear that the line of sight must be dominated by concentrations of gas, hot or cold, with electron densities considerably in excess of 0.05 cm^{-3} . When allowance is made for a continuum optical depth of unity due to an intervening H II region or a high-density cold cloud which make a negligible contribution to τ_L at 111 MHz, the upper limits on η are still only 0.02 and 0.15 for $N_e = 0.05 \text{ cm}^{-3}$ and $T_e = 20^\circ \text{K}$ and 100°K respectively.

More stringent limits on the filling factor for the cold cloud component can be imposed if the second and third terms in Eq. (1) are included in the analysis. The galactic background (T_M) in particular is the dominant factor in the 111 MHz observations, and the average upper limit on the ratio $\Delta T_L/T_M$ for the four sources listed in Table 1 is 0.005; for $T_e = 20^\circ \text{K}$, $N_e = 0.05 \text{ cm}^{-3}$, and an assumed total path length of 10 kpc this implies $\eta < 0.001$, using a procedure similar to that employed above. It is assumed here that the cold clouds are uniformly mixed with the nonthermal galactic emission, and dilution effects due to the geometry of the galaxy have been ignored; for these reasons the limit $\eta < 0.001$ is probably somewhat too low, and the correct upper limit on the filling factor likely lies somewhere between this value and the more conservative ones given above.

III. The High-density Gas

The fact that no low-frequency line emission is detected from the high-density gas responsible for the observed low-frequency continuum absorption in Sgr A and W49B permits limits to be placed on its density and filling factor, and the implied ionization rates. Figure 3 shows the ratio τ_L/τ_C , computed from Eqs. (2) and (3), plotted against density for $\nu = 111 \text{ MHz}$, $\Delta V_L = 30 \text{ km/s}$, and a range of electron temperatures. Upper limits on this ratio can be computed from Eq. (4) for W49B and Sgr A, using the continuum optical depths (0.22 and 2.9 respectively) determined by Dulk and Slee (1975), and the upper limits on $\Delta T_L/T_O$ (0.080 and 0.063 respectively from Table 1) based on the Heiles and Turner (1971) observations. These limits are indicated in Fig. 3; they imply lower limits on the electron density of $0.2\text{--}2 \text{ cm}^{-3}$, depending on the temperature assumed. The filling factor η and ionization rate $\zeta \text{ (s}^{-1}\text{)}$ can then readily be computed for these densities from the emission measures, and from the ionization equilibrium equation (Spitzer, 1968),

$$\zeta N_{\text{H I}} = N_e N_{\text{H II}} \alpha^{(2)}, \quad (5)$$

where $\alpha^{(2)} \text{ (cm}^3 \text{ s}^{-1}\text{)}$ is the hydrogen recombination coefficient for all levels down to the second, for a given temperature. The results are summarised in Table 2.

There are three major possible sources of error in this analysis: the theoretical b_n -factors, the assumed line widths, and the measured continuum optical depths. The

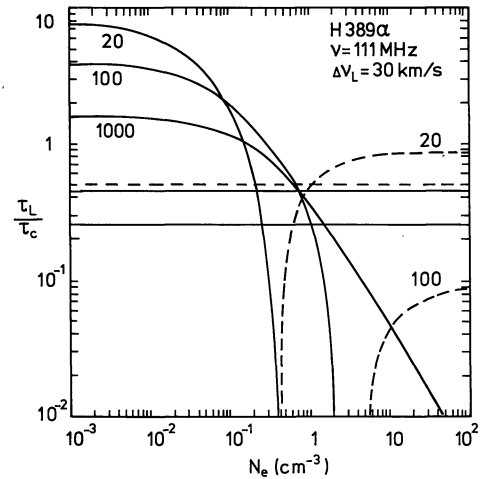


Fig. 3. The ratio of H389 α line and 111 MHz continuum optical depths computed from Eqs. (2) and (3) for $\Delta V_L = 30 \text{ km/s}$, plotted against electron density for three values of electron temperature, 20, 100 and 1000°K . The solid and dashed curves denote negative and positive line optical depths respectively. The upper and lower horizontal solid lines indicate upper limits on the value of $-\tau_L/\tau_C$ as deduced from observations of W49B and Sgr A respectively, and the horizontal dashed line indicates a similar upper limit for $+\tau_L/\tau_C$ in the case of W49B (there is no upper limit on $+\tau_L/\tau_C$ in the case of Sgr A)

crucial factors $d \ln b_n / d n$ scale approximately linearly with N_e over the range of values considered here, and should be accurate within a factor of two (Paper I; see Fig. 2). ΔV_L and τ_C are linearly proportional to the ordinate of Fig. 3; at $\tau_L/\tau_C = 0.3$, a 10-fold error in either will therefore produce a 2, 4 and 20-fold error in N_e for $T_e = 20, 100$ and 1000°K respectively. The derived density is therefore relatively insensitive to errors in ΔV_L and τ_C , especially at low temperatures. The assumed line width of 30 km/s is unlikely to be in error by more than a factor of two or three, and the measured optical depths should be accurate at least within 50% (Dulk and Slee, 1975). The maximum possible error in N_e should therefore not exceed a factor of 3, 4 and 8 for $T_e = 20, 100$ and 1000°K respectively.

It is evident from Table 2 that the high-density gas along the line of sight must be highly clumped if the temperature is low. The densities and ionization rates are substantially higher than those believed to prevail

Table 2. Derived properties of the dense component

T_e ($^\circ \text{K}$)	20	100	1000
Sgr A			
$N_e \text{ (cm}^{-3}\text{)}$	> 0.3	> 1	> 2
η	< 0.03	< 0.02	< 0.09
$\zeta N_{\text{H I}} \text{ (} 10^{-12} \text{ cm}^{-3} \text{ s}^{-1}\text{)}$	> 2	> 7	> 6
W49B			
$N_e \text{ (cm}^{-3}\text{)}$	0.2–1.0	> 0.7	> 0.7
η	0.0002–0.005	< 0.003	< 0.06
$\zeta N_{\text{H I}} \text{ (} 10^{-12} \text{ cm}^{-3} \text{ s}^{-1}\text{)}$	0.8–20	> 3	> 0.7

in the solar neighborhood (Field *et al.*, 1969; Hjellming *et al.* 1969); higher-frequency recombination line observations also indicate higher interstellar electron densities in the inner regions of the galaxy (Gordon, 1972; Jackson and Kerr, 1971; Lockman and Gordon, 1973; Matthews *et al.*, 1973). Torres-Peimbert *et al.* (1974) have recently shown that distributed OB stars may be responsible for most of this ionization, the observed low-frequency continuum absorption of Sgr A and W49B may therefore be due to diffuse H II regions.

IV. Conclusions

Low-frequency recombination line observations provide a method of determining simultaneously the density of, and path length through, cold, low-density interstellar plasmas. This preliminary study indicates (1) that the cold cloud component occupies only a small fraction of the volume of interstellar space ($\eta < 0.005-0.05$), and (2) that the gas responsible for the low-frequency continuum absorption of W49B and Sgr A is characterized by electron densities exceeding $0.2-2 \text{ cm}^{-3}$.

Acknowledgements. I am most grateful to V. Radhakrishnan, D. C. V. Mallik, S. R. Pottasch and the referee for helpful comments and criticisms.

References

- Dulk, G. A., Slee, O. B. 1975, *Astrophys. J.* **199**, 61
 Field, G. B., Goldsmith, D. W., Habing, H. J. 1969, *Astrophys. J.* **155**, 149
 Gayet, R. 1970, *Astron. & Astrophys.* **9**, 312
 Gordon, M. A. 1972, *Astrophys. J.* **174**, 361
 Heiles, C. E., Turner, B. E. 1971, *Astrophys. Letters* **8**, 89
 Hjellming, R. M., Gordon, C. P., Gordon, K. J. 1969, *Astron. & Astrophys.* **2**, 202
 Jackson, P. D., Kerr, F. J. 1971, *Astrophys. J.* **168**, 29
 Lockman, F. J., Gordon, M. A. 1973, *Astrophys. J.* **182**, 25
 Matthews, H. E., Pedlar, A., Davies, R. D. 1973, *Monthly Notices Roy. Astron. Soc.* **165**, 149
 Maxwell, A., Taylor, J. H. 1968, *Astrophys. Letters* **2**, 191
 Milne, D. K. 1970, *Australian J. Phys.* **23**, 425
 Oster, L. 1961, *Rev. Modern Phys.* **33**, 525
 Oster, L. 1970, *Astron. & Astrophys.* **9**, 318
 Radhakrishnan, V., Goss, W. M., Murray, J. D., Brooks, J. W. 1972, *Astrophys. J. Suppl.* No. 203, 49
 Shaver, P. A. 1975, *Pramana* **5**, 1
 Spitzer, L., Jr. 1968, *Diffuse Matter in Space*; Interscience, New York
 Torres-Peimbert, S., Lozano-Aranjo, A., Peimbert, M. 1974, *Astrophys. J.* **191**, 401
 Turner, B. E., Heiles, C. E., Scharlemann, E. 1970, *Astrophys. Letters* **5**, 197
 Wilson, T. L. 1973, *Astron. & Astrophys.* **25**, 329

P. A. Shaver
 Kapteyn Astronomical Institute
 P.O. Box 800
 NL-8002 Groningen, The Netherlands